Modelling and Experimental Study of a Wind Turbine System in Hybrid Connection with Compressed Air Energy Storage

Christopher Krupke, Jihong Wang* (*Senior Member, IEEE*), Jonathan Clarke and Xing Luo (*Member, IEEE)*

***Abstract*—The paper presents a new hybrid wind turbine system that is formed by a continuously variable transmission connection of the turbine drive shaft with an air expander/compressor. A mechanical power split device is designed to synthesize the power delivered by the wind turbine and the air expander/compressor. A small scale hybrid wind turbine system is mathematically modelled, analyzed and validated using a laboratory-scale experimental test rig. By utilizing compressed air energy storage it is shown that the hybrid wind turbine system can provide smooth power output under fluctuating wind speed conditions. Such a direct connection structure reduces the overall system cost by using one generator instead of two compared with the conventional CAES system structure. The study demonstrates the benefit of improved efficiency and flexibility brought to the turbine operation by the hybridization of wind energy and stored energy.**

I. INTRODUCTION

Increased electricity generation from wind energy sources is considered as one of the top priority strategies worldwide for reducing CO_2 emissions and maintaining sustainable economic development. However, increased exploitation of wind power poses challenges for power network operation, due to the nature of unpredictability and variability of wind power [1, 2]. To address the challenge, various methods are under investigation, such as super-grids, flexible operation of power plants, demand-side response management, interconnectors and Energy Storage (ES). Among all the potential solutions, ES is recognized as one of the feasible options for decoupling the fluctuating power supply from the load demand.

Apart from pumped hydro, batteries, hydrogen, flywheels and capacitors for energy storage, Compressed Air Energy Storage (CAES) is a well-known, controllable and affordable technology [3]. In a CAES system, electric power is used to compress air for storing high pressure air in a vessel or a cavern and the energy stored can be called into use to generate electricity when needed. Compared with other types of ES technologies, CAES is sustainable, does not produce chemical waste and is suitable for various scales of storage. CAES is already considered to facilitate wind power and to compensate for the power supply fluctuations [4-6]. Study on the integration of intermittent renewable energy with CAES is reported in [7-10] to investigate economic profit optimization. Mathematical modelling study and economic analysis were carried out in [11-14]. In order to increase flexibility and to provide smooth power output from renewable energy sources, technologies for wind power integration were investigated such as wind-diesel systems [15, 16], wind turbines with hydraulic and pneumatic pumps [17] or hybrid wind turbines in connection with compressed air and super-capacitors [18]. A scroll type air expanders in connection with the wind turbine drive shaft to realize direct integration of CAES with wind power generation is suggested in [19-21].

In this paper, a wind turbine system in hybrid connection with CAES is proposed, in which a scroll type air expander/compressor and a mechanical power split device are combined to engage CAES to the turbine powertrain. Smoother power generation is achieved as the air expander provides additional power from CAES when wind speed is not high enough to maintain the balance between the power demand and power supply. In the time period of power oversupply, the excess power can be used to compress air for storage. It is also anticipated that such a hybrid structure may help reduce the mechanical strain on the turbine drive train induced by undesired wind gusts. In this paper, the study focuses on a few kW small scale hybrid wind turbine in order to demonstrate the proposed concept on a laboratory based test rig. The dynamic mathematical model is developed for the whole system and simulation study is conducted. A small test system is implemented in the research laboratory to verify the modelling and simulation study outcomes. The study shows that this hybrid system is feasible from the technology point of view. With a suitably designed control strategy the system delivers smooth power output under fluctuating wind speed conditions. Compared with the work published in [19, 20], the main new contribution of this paper is that a new mechanical power transmission structure is proposed. A power split device is introduced to achieve continuous and smooth switching to the hybrid connection and different operating modes. The study in [21] investigates the energy discharge operating mode only (air expansion). The mechanical structure presented in this study enables a single scroll air expander/compressor unit to work either as an air expander or an air compressor, so that a complete cycle of charging and discharging the store is achieved. The whole system experimental test and system analysis are also provided in this paper.

The authors would like to thank the funding support from Engineering Physics and Science Research Council (EPSRC), UK (EP/K002228/1) the research studentship support from EPSRC DTA and the School of Engineering, the University of Warwick, and give their thanks to the support from China 973 Research Programme (2015CB251301) to enable the collaboration in realization of the experimental system. Further acknowledgement goes to Dr Oleh Kiselychnyk for the support in mathematical modelling and Dr Ken Mao, Professor JiDai Wang and Dr Zhiwei Wang for advice on gear box design and the extensive support in the manufacturing process of the device.

C. Krupke, Jonathan Clarke and Xing Luo are with the School of Engineering, the University of Warwick, Coventry CV4 7AL, UK

*J Wang, the author for correspondence, is with School of Engineering, the University of Warwick, Coventry CV4 7AL, UK and also a Guest Professor of Huazhong University of Science and Technology, PR China jihong.wang@warwick.ac.uk, jihongwang@hust.edu.cn.

The paper is organized into six sections. Section II describes the whole system structure. The mathematical modelling and simulation of the system is given in Section III. In Section IV, the experimental test rig set up and model validation are presented. System analysis and energy efficiencies are studied in Section V. Concluding remarks are given in Section VI.

II. Description of the System Structure

In general, a CAES system has a process from electricity to electricity. Electric motors power compressors to produce compressed air for storage and the stored compressed air can be called into use to power an air turbine to drive a generator for electricity generation. The case of the electricity generated by wind power with integration of CAES is illustrated in Figure 1a). The early research work at Warwick University, reported in [19, 20], proposed a hybrid wind turbine system which has a different configuration and is described in Figure 1b). It can be seen that the proposed system structure connects an air expander to the wind turbine shaft via a clutch. The wind turbine generator is used for wind power generation and also CAES conversion. Such a system structure requires a complex control strategy to ensure that the air expander is engaged only when its rotational speed is synchronized with the drive shaft's speed. The results in [19, 20] show that torque can be added to the turbine drive shaft and, hence, the power output is increased. On the other hand, the added torque also leads to a propelled turbine rotor, which can have negative effects on the turbine's efficiency. In addition, the expander cannot be used as a compressor to compress air in the case that excess power is produced by the wind.

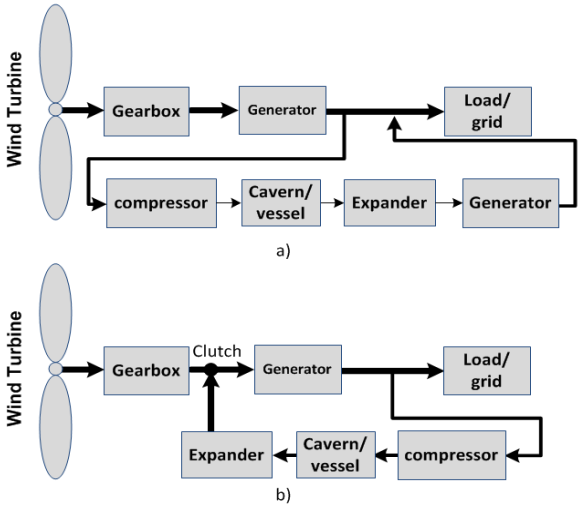

Figure 1: a) general CAES operation. b) Early version of the Hybrid Wind Turbine System

Following the work reported in [19, 20], a new system structure is proposed in this paper by introducing a Power Split Device (PSD). The system topology is shown in Figure 2 with a planetary gear box as the PSD. The PSD merges the torques from the turbine rotor shaft, the scroll air expander/compressor and the generator. The planetary gear box consists of a ring gear, connected to the generator, a planet carrier, connected to the wind turbine, and a sun gear to be connected to the scroll air expander/compressor. Power can continuously be added from CAES via the air expander, meaning the air expander can be utilized in its entire speed range and is not tied to the rotational speed of the drive train. The air expander can also be driven backwards (which makes it work as a compressor) in the time of excess wind power generation over the demand. This was not possible in the previous study [19, 20]. Having this system structure, a single device can serve as either compressor or expander for charging (compression) and discharging (expansion) processes, respectively. In addition, the generator can also work as a motor, driving the scroll compressor, while the wind turbine is locked against spinning backwards. Therefore, the store can also be charged by taking electricity from the grid.

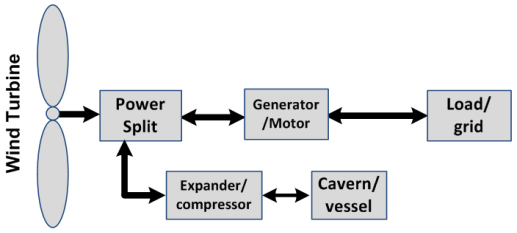

Figure 2: Illustration of the Hybrid Wind Turbine Topology

III. Mathematical Modelling of the Whole System

In this section, the dynamic mathematical model of the whole system is presented including the scroll air expander, the wind turbine, the generator and the power split device. The modelling of the individual system components is explained first, which covers their operating principles and mathematical model derivation. Table II shows the system parameters, which were obtained from product data sheets or via parameter identification using Genetic Algorithms. The models of the components are then linked together to form the whole hybrid wind turbine system model. In this paper, due to page limits, only the work for the discharging process is presented in which the scroll unit works as an air expander. The charging process/compression stage will be discussed in further publications.

A. Model of Horizontal Axis Wind Turbines

The wind turbine's power output is characterized by Eq. (1) [22].

$$P_{turbine} = 0.5\rho A v^3 c_p(\lambda) \quad (1)$$

where $P_{turbine}$ is the turbine's mechanical power output, ρ is the air density, A is the rotor disc area, v is the wind speed and c_p is the turbine power coefficient. The c_p is of particular importance since it describes how much mechanical power can be extracted from the incoming aerodynamic power. The c_p is a function of the tip speed ratio λ, i.e. the ratio between the tangential speed of the rotor blades and the incoming wind speed. In theory, an optimum c_p can be found for any wind turbine at a given wind speed. However, the c_p calculation requires aerodynamic knowledge about the airfoil and can be described numerically. Eq.(2) shows the chosen c_p calculation, while the pitch angle is set to zero for the small scale wind turbine [22].

$$c_p(\lambda) = 0.24\left(\frac{78}{\lambda_i} - 5\right)e^{-\frac{10.5}{\lambda_i}} + 0.02\lambda \quad (2)$$

with λ_i being an auxiliary variable:

$$\frac{1}{\lambda_i} = \frac{1}{\lambda} - 0.035 \quad (3)$$

B. Model of Permanent Magnet Synchronous Generator

The Permanent Magnet Synchronous Generator (PMSG) can be modelled in the *DQ* reference frame, described by Eqs.(4) and (5) and is based on [23].

$$\dot{u}_d = \frac{R_l}{L}\left(-u_d\left(1 + \frac{R_s}{R_l}\right) + \omega_{gen} L p \frac{u_q}{R_l}\right) \quad (4)$$

$$\dot{u}_q = \frac{R_l}{L}\left(-u_q\left(1 + \frac{R_s}{R_l}\right) - \omega_{gen} L p_n \frac{u_d}{R_l} + \omega_{gen} p \psi\right) \quad (5)$$

with u_d, u_q being the induced voltages in *DQ* coordinates when a driving torque is applied. $R_s, R_l, \omega_{gen}, L, p_n$ and ψ are stator resistance, load resistance, rotational speed of the generator shaft, inductance, number of pole pairs and the magnetic flux, respectively. Note that only resistive load is used in this description. The torque is proportional to the current, number of poles and flux, see Eq.(6).

$$\tau_{gen} = \frac{3}{2} p_n \psi i_q = \frac{3}{2} p_n \psi \frac{u_q}{R_l} \quad (6)$$

with i_q being the current in the *q* axis.

C. Model of Scroll Air Expander

Scroll type compressors can be found in refrigerators or air conditioning systems in vehicles. The design structure can also be used for air expanders and has recently attracted researchers and industry for applications such as Uninterrupted Power Supply systems (UPS), ranging from a few kW up to 50 kW power rating [24]. It can also be found in applications for waste heat recovery systems [25]. A scroll air expander consists of two spirals - a fixed and a moving spiral. The moving spiral is connected to a crankshaft, allowing for eccentric motion, while following a fixed path with respect to the fixed spiral. While orbiting, the chamber volumes between the fixed and the moving spiral are increasing. The process repeats with every 360° rotation.

Comprehensive modelling study is reported in [26, 27], ranging from the geometry study to thermodynamic and mechanical analysis. Therefore, the entire derivation of the scroll air expander model will not be repeated in this paper and a brief description of the key components will be given. The scroll air expander used in this study is a Sanden TRSA09 compressor with 2.1 wraps, modified in-house to serve as an expander. Figure 3 shows a function block diagram of the scroll air expander model. As the expander shaft rotates, the volumes in central, side and exhaust chambers are computed. The pressure and temperature inside the chambers can be derived based on the volumes, the inlet air pressure and inlet air temperature. The pressure difference across adjacent chambers induces the driving torque, which leads to rotation depending on the load. The chamber pressures are linked to the air mass flow rate, the rate of volume changes, chamber air temperature and the current pressure state, described in Eqs.(7-9).

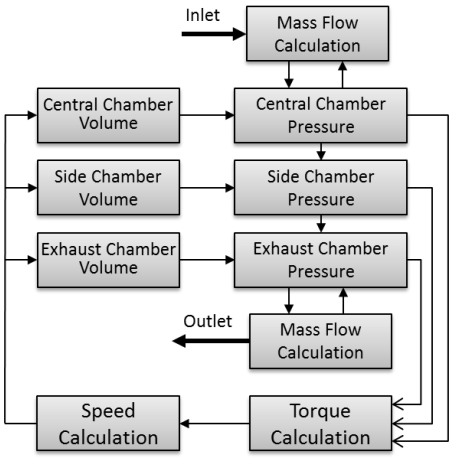

Figure 3: Function Block Diagram of Scroll Air Expander

The equations are simplified to have a constant temperature due to the fact that temperature changes have only a minor effect on the torque/speed characteristic of the expander in low pressure regions (1 to 5bar) from our experiments.

$$\dot{p}_c = \frac{1}{V_c}\left(\dot{m}_c R T_c - \dot{V}_c p_c\right) \quad (7)$$

$$\dot{p}_s = \frac{1}{V_s}\left(-\dot{V}_s p_s\right) \quad (8)$$

$$\dot{p}_e = \frac{1}{V_e}\left(\dot{m}_e R T_e - \dot{V}_e p_e\right) \quad (9)$$

where p is the chamber air pressure; V is the chamber volume; T is the temperature inside each chamber; $\dot{m}$ is the mass flow rate of air into the central chamber and out of the exhaust chamber; R is the gas constant. The subscripts *c*, *s* and *e* stand for central chamber, side chamber and exhaust chamber, respectively. The mass flow rate is derived from the orifice theory and can be described with the following formula:

$$\dot{m}_i = A_i \frac{c_d c_0 p_u}{\sqrt{T}} f(p_u, p_d) \quad (10)$$

with c_d, c_0 being discharge and flow constants and p_u and p_d the upstream and downstream pressure across the orifice. A_i is the smallest cross-sectional area of the inlet and outlet, respectively. Furthermore, $f(p_u, p_d)$ is defined as follows:

$$f(p_u, p_d) = \begin{cases} 1 & , \frac{p_d}{p_u} \le c_r \\ c_k\left(\left(\frac{p_d}{p_u}\right)^{\frac{2}{k}} - \left(\frac{p_d}{p_u}\right)^{\frac{k+1}{k}}\right)^{\frac{1}{2}} & , \frac{p_d}{p_u} < 1 \end{cases} \quad (11)$$

with c_k, k and c_r being constants (see Table II).

The total torque produced by the scroll air expander depends on the pressure difference across adjacent chambers and is represented by Eq.(12) [26].

$$\tau_{scroll} = \sum hr(2\rho_0 + 2k_s\alpha + (4j+1)k_s\pi)\Delta p \qquad (12)$$

where h is the depth of the scroll; r is the radius of the orbit; Δp is the pressure difference between adjacent chambers; ρ_0 is the initial radius of curvature; k_s determines the shape of the spiral; α is the orbit angle and j increases from 0 to the number of side chamber pairs. The detailed method for calculating the chamber volumes can be found in [27].

In order to investigate the scroll air expander's efficiency, the ratio between power in compressed air flow and mechanical power must be established. The power in compressed air flow can be computed according to Eq.(13) [28].

$$P_{air} = p\dot{V}ln\left(\frac{p}{p_a}\right) = p_a\dot{V}_a \ln\left(\frac{p}{p_a}\right) \qquad (13)$$

The subscript a stands for atmospheric conditions. The scroll air expander efficiency is defined as follows:

$$\mu_{scroll} = \frac{P_{mech}}{P_{air}} = \frac{\tau_{scroll}\omega_{scroll}}{P_{air}} \qquad (14)$$

D. Model of the Power Split Device

The power split device used in this application is a single-stage planetary gear box, consisting of three components: a sun gear, a planet carrier and a ring gear. In general applications of planetary gear boxes, one of the three components is fixed. However, in this application all three components are movable. The sun gear is connected to the scroll air expander/compressor, the planet carrier to the turbine and the ring gear to the generator. The main torque input is provided by the wind turbine while the scroll air expander transfers torque to the generator via the planet carrier, meaning that the turbine experiences a higher load torque. The scroll air expander can also become driven, which turns it into a compressor.

Based on the lever analogy in [29], the dynamic mathematical model can be developed. From Figure 4, the sun gear (S) is driven by the scroll air expander's torque τ_{air}, reduced by its friction components $\tau_{fr,air}$ and gear box friction $\tau_{fr,gear,s}$. The planet carrier (C) is driven by the turbine torque.

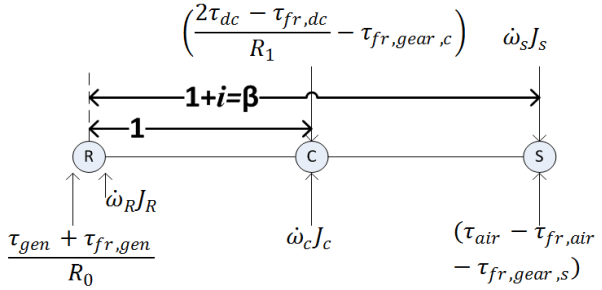

Figure 4: Lever Diagram for Power Split Device

Since the test rig utilizes 2 DC motors as a turbine emulator, the DC motor torque τ_{dc} is denoted. It is reduced by its drive shaft friction $\tau_{fr,dc}$ and gear box friction $\tau_{fr,gear,c}$. The generator is connected to the ring gear (R), taking into account the friction $\tau_{fr,gen}$. R_0 and R_1 are transmission ratios of the drive train, whereas i is the gear box transmission ratio from sun to ring gear and $\dot{\omega}_i$ describes the respective rotational acceleration of the gear components.

Based on the physical model in Figure 4, two differential equations can be derived that describe the system. The sum of momentums is arbitrarily taken around the sun and ring gear, respectively.

$$\sum \tau^{sun} = 0 = -(\beta - 1)\left(\frac{2\tau_{dc} - \tau_{fr,dc}}{R_1} - \tau_{fr,gear,c}\right) + (\beta - 1)\dot{\omega}_c J_c + \beta\frac{\tau_{gen} + \tau_{fr,gen}}{R_0} + \beta\dot{\omega}_R J_R \qquad (15)$$

$$\sum \tau^{ring} = 0 = \left(\frac{2\tau_{dc} - \tau_{fr,dc}}{R_1} - \tau_{fr,gear,c}\right) - \beta(\tau_{air} - \tau_{fr,air} - \tau_{fr,gear,s}) - \dot{\omega}_c J_c + \dot{\omega}_s J_s \beta \qquad (16)$$

The kinematics of the gear box is illustrated in Figure 5.

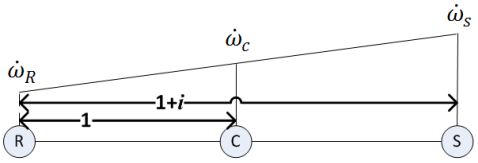

Figure 5: Power Split Kinematics

Using the theorem of intersecting lines, the following relationship can be derived:

$$\dot{\omega}_R = \frac{\dot{\omega}_c(1+i)}{i} - \frac{\dot{\omega}_s}{i} \qquad (17)$$

Substituting Eq.(17) into Eqs.(15) and (16), and decoupling the equations from each other with respect to $\dot{\omega}_c$ and $\dot{\omega}_s$, the following differential equations hold:

$$\dot{\omega}_c = \frac{1}{J_{k2}}[\left(\frac{2\tau_{dc} - \tau_{fr,dc}}{R_1} - \tau_{fr,gear,c}\right)J_{k3} - (1+i)\cdot (\tau_{air} - \tau_{fr,air} - \tau_{fr,gear,s}) + J_{k4}\left(\frac{\tau_{gen} + \tau_{fr,gen}}{R_0}\right)] \qquad (18)$$

$$\dot{\omega}_s = \frac{1}{J_{k5}}[\left(\frac{2\tau_{dc} - \tau_{fr,dc}}{R_1} - \tau_{fr,gear,c}\right)J_{k6} + (1+i)\left(\frac{\tau_{gen} + \tau_{fr,gen}}{R_0}\right) - \frac{J_k}{J_c}(i+i)(\tau_{air} - \tau_{fr,air} - \tau_{fr,gear,s})] \qquad (19)$$

with J_{k_i} being composed terms of inertias (see Table III).

E. Whole System Model

All the system component models are connected and controlled via a PID controller to form a complete closed-loop system as shown in Figure 6. The paper focuses on system modelling and analysis, so only a conventional PID

controller is discussed that regulates the scroll air expander power and, in turn, the generator's power output. The control action is realized by controlling the air pressure input of the scroll air expander for which a pressure regulator can be used. As stated in the previous section, only the *air expander* stream is discussed in this paper, that is, the power from CAES can be added to the system via the air expander.

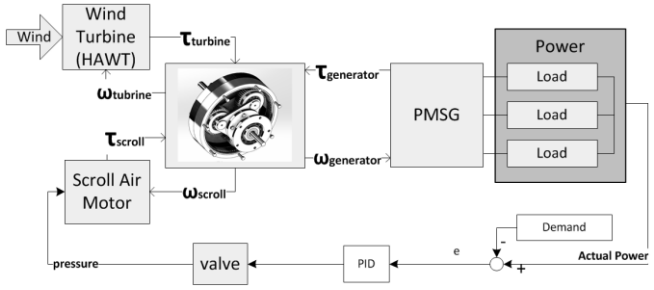

Figure 6: Control Schematic

IV. Experimental Test System

An experimental test rig was set up to validate the developed models and to find parameters for the components used in the system. A 1kW PMSG and a 2.1-wraps scroll air expander/compressor are employed in the experimental system. The gear box was designed with a gear ratio of 5 (from sun to ring gear) to match the component's torque/speed characteristics. Due to limitations of acquiring a suitable real small-scale wind turbine, two DC motors are employed to form an emulator of a small scale horizontal axis wind turbine in the test system.

A. Test Rig Set Up

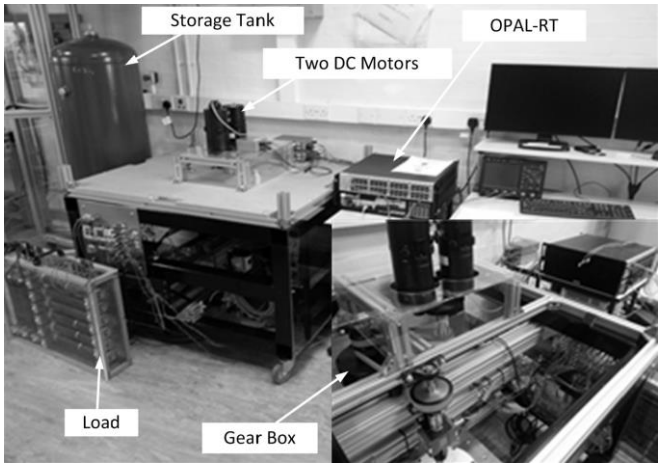

Figure 7: Hybrid Wind Turbine Test Rig Set Up

The test rig comprises a metal frame hub (see Figure 7) that carries the generator, the scroll air expander, the gear box and measurement instruments as well as actuators. The DC motors (turbine emulator) are connected to a shaft on top of the hub, which also provides the opportunity to connect it to a real wind turbine for future tests. All sensor outputs are connected to an Opal-RT Real-Time Hardware, which interfaces with Matlab/Simulink and with which data are acquired and the test rig is controlled at the sampling period of 1 ms. Table I shows the main system components.

TABLE I. Test Rig Components

Component	*Description*
Generator	Ginlong Technologies GL-PMG 1000
Scroll air expander	Sanden TRS090
2 DC motors	Callan Technology M4-2952
2 DC amplifiers	20/100 20A 100V Analogue Amplifier
Real-Time Target	Opal OP5600 digital simulator with RT-lab
Pressure valve	Festo MPPE-3-1/4-10-010-B (0-10bar)
Encoder for DC motors	British Encoder Production, Type: 260/1/HV 1000PPR
2 Torque and speed sensors	TorqSense RWT410/420 Series Transducer
Pressure Sensor	Festo Pressure sensor SDE1-D10-G2-W18-L-PU-M8
Flow Sensor	Festo MS6-SFE
Voltage Sensor	LEM - LV 25-P - Voltage Transducer, PCB - LV 25-P
Current Sensor	LEM - LTS 6-NP - Current Transducer, 6A, PCB - LTS 6-NP

B. Model validation

The test rig is used to validate the system's components individually followed by testing the whole hybrid wind turbine system. Unknown parameters were identified by manual searching methods and Genetic Algorithms. The detailed parameter identification is not given in this paper due to the restriction of the number of pages. For the comparison between simulation and experimental results and for achieving a better representation of the system dynamics, random voltage and inlet air pressure profiles for the DC motors and the scroll air expander are used as input signals, as shown in Figure 8.

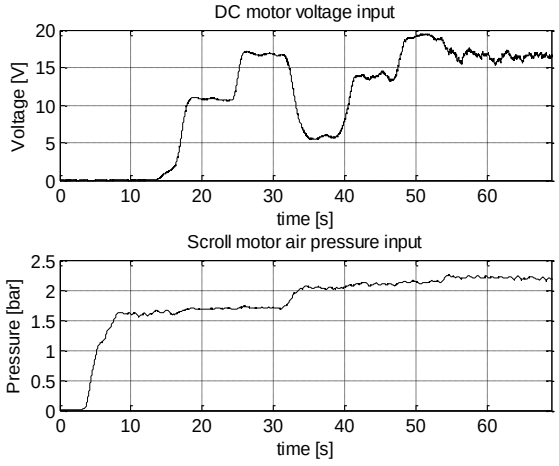

Figure 8: Voltage and Air Pressure (gauge) Input

The input voltages and air pressures applied to the test rig were recorded and then used as inputs for the simulation study. The corresponding torque and speed of the DC motors, the air expander and the generator are recorded. Figure 9 shows the comparison of the torque profiles between the simulated and experimental results.

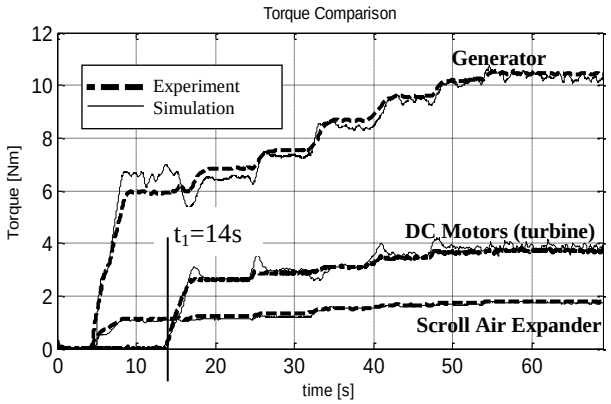

Figure 9: Torque Comparison Simulation and Experimental Test

A good fit between the simulation and experimental test results is observed. The scroll air expander drives the generator by itself until t_1, that is, the power output comes from CAES only. From t_1, the DC motors (wind turbine) are engaged and the generator torque is increased, meaning that both wind power and power from CAES are merged to drive the generator.

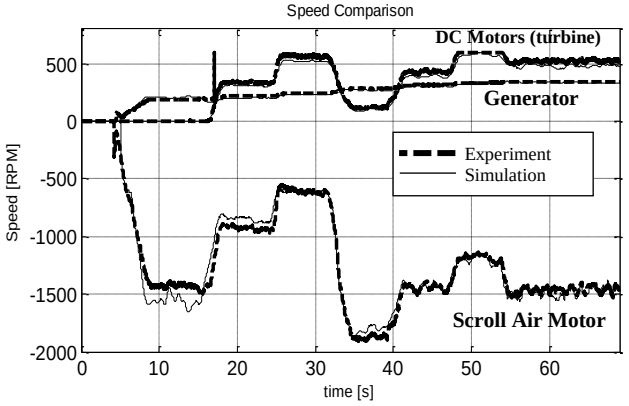

Figure 10: Speed Comparison Simulation and Experimental Test

Figure 10 shows the rotational speed of each component. It can be seen that the scroll air expander spins in the opposite direction compared to the generator and the DC motors. The scroll air expander's speed changes significantly within the first 30sec although the air pressure is kept nearly the same. This is due to the DC motors, which become engaged and add torque to the system. Therefore, Figure 9 and 10 illustrate the interaction between the system components and applied torques well.

V. Simulation Study and Analysis

A. Operating Scenarios

The mathematical model of the hybrid wind turbine is validated in Section IV, so that it can be used to investigate the effects of engaging compressed air energy through the direct mechanical transmission connection. Extensive simulation study is conducted in this section. Firstly, a 2.5m diameter standalone Horizontal Axis Wind Turbine (HAWT) is tested, i.e. the direct connection from the wind turbine to the generator without the interaction of the scroll air expander. The wind speed scenario and the corresponding power of the HAWT are shown in Figure 11. The wind speed scenario is obtained from the published data in [30].

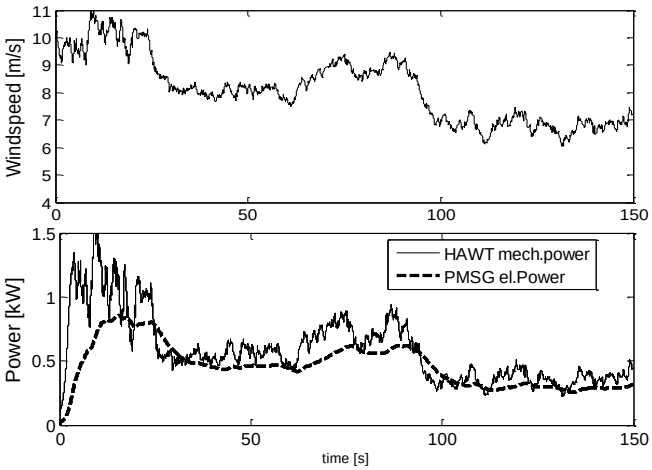

Figure 11: Wind Speed and Standalone HAWT Power

For comparison, Figure 12 shows the simulation results for the power generation from the same HAWT in hybrid connection with the scroll air expander. In this case, the power output is controlled to meet 1kW demand for the first 100s and 0.75kW for the remaining 50s, which is introduced with a step change in power demand. The same wind speed profile from Figure 11 is used for this simulation.

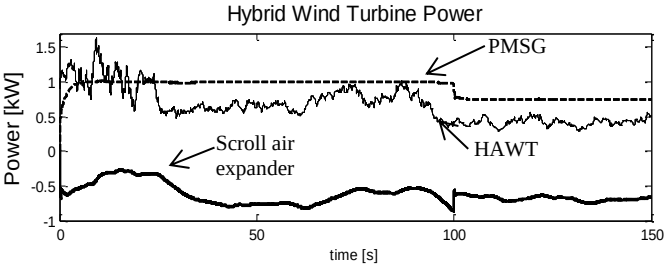

Figure 12: Hybrid Wind Turbine Power and Efficiency

The scroll air expander engages and adds power to the system, so that the power demand is met. It is noticed from Figure 12 that the scroll air expander's power has a negative sign, which is because the scroll air expander rotates in the opposite direction with respect to the HAWT and the PMSG through the gear box. When the HAWT and the scroll air expander work together, the torque added from the scroll air expander to the PSD influences the HAWT's power coefficient positively as shown in Figure 13. The increase of the HAWT's power coefficient c_p is observed because the HAWT operates at a more efficient tip speed ratio in comparison to the standalone HAWT under the same wind speed conditions. Therefore, not only can power be added continuously to the system, it also has a beneficial effect on the HAWT's power coefficient.

Since the scroll air expander applies torque via the wind turbine, four scenarios can occur: 1) The wind speed is too low, the turbine does not rotate; the scroll air expander drives the generator by itself and the turbine rotor must be

secured from spinning backwards. 2) The HAWT generates power in standalone mode. 3) The wind speed is not high enough and CAES needs to be employed to add additional power to generate the desired power output. 4) The wind turbine produces too much power, which can be used to compress air for storage.

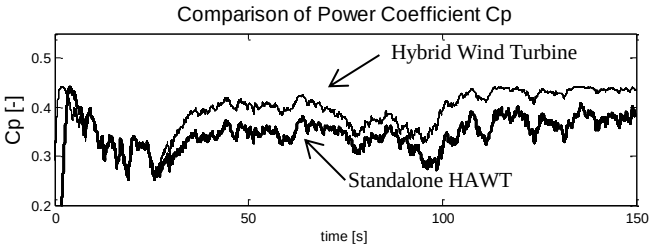

Figure 13: Comparison of Power Coefficient C_p

B. *Efficiency Analysis*

The round-trip efficiency of the hybrid wind turbine is defined as the ratio between the electric energy generated and the HAWT's mechanical energy, after all energy has passed through storage. The energy transfer from the HAWT to storage is demonstrated in Figure 14.

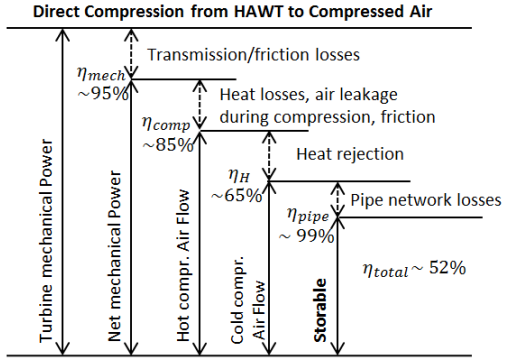

Figure 14: Energy Transfer from HAWT to Compressed Air

For the process, four major energy losses are identified which are shown in Figure 14. The associated energy efficiencies are also listed in the figure and are estimated with references to the work in [31-34]. The overall compression process efficiency from the HAWT's mechanical energy to compressed air energy is estimated to 52%. The energy transfer from the stored energy to electric energy is shown in Figure 15.

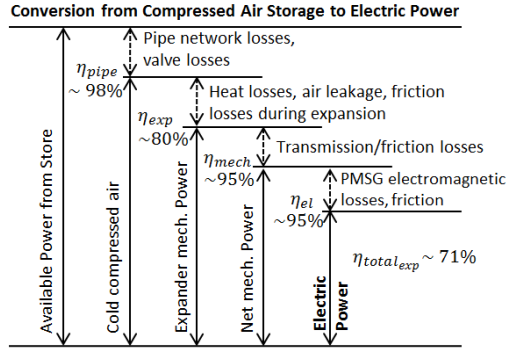

Figure 15: Conversion from Compressed Air Storage to Electric Power

Similar to the compression process, the major losses are identified and shown in Figure 15. The estimated efficiency for the expansion process is around 71% [31, 33]. Therefore, the round-trip efficiency is approximately $0.52 \cdot 0.71 \cdot 100\% \approx 37\%$. A number of research projects are on-going worldwide aiming at improving energy efficiency of CAES systems. With the recently reported development of CAES technology, the round-trip efficiency (electricity to electricity) of 53% is achieved for a 1MW Adiabatic-CAES demonstration plant [35].

VI. Concluding Remarks

In this paper, a new hybrid wind turbine system is presented that uses CAES and a power split device with the aim of smoothing power output under fluctuating wind speeds. The power split device merges the torques from the scroll air expander/compressor, the wind turbine and the generator. A mathematical model is derived based on a small scale hybrid wind turbine system and is successfully validated by comparing the experimental and simulation results.

The system structure proposed in the paper is more cost effective as only one generator is required and the expander can be operated reversibly as a compressor for both charging and discharging processes. The proposed hybrid wind turbine can regulate the power output and help follow the demand profile via controlling the charging and discharging processes. This is particularly useful to the distributed and isolated power grid. Especially remote areas with poor power network connections, but rich in wind energy resources, will benefit from the hybrid wind turbine system. Furthermore, the study has also demonstrated that the wind turbine power coefficient c_p can be improved by the structure of the direct mechanical engagement of the scroll air expander with the turbine shaft. Additionally, the hybrid set up would allow for damping shock loads from wind gusts, which may play a positive role in prolonging the life-time of the wind turbine gear box and reducing the cost of maintenance.

The work reported in this paper is based on the study of a small scale wind turbine system. A preliminary study has been conducted by the authors concerning a 1MW hybrid wind turbine for which two screw expanders/compressors are utilized. The initial study indicates that the system is feasible from the mechanical transmission point of view. However, more extensive study regarding a MW scale hybrid wind turbine is required before any firm conclusion can be drawn. The work is ongoing and will be reported in future publications. In collaboration with British Geological Survey, the authors are currently working on investigating the CAES potential in the UK [36]. From the study it is shown that the UK has the potential to form salt caverns to store compressed air energy of over 1000 GWh.

APPENDIX A

TABLE II. SYSTEM PARAMETERS

Parameter	Value	Parameter	Value
General		***Generator***	
T	293 K	R_s	6ohm
c_0	0.0404	R_l	64ohm
c_d	0.8	L	17.5mH
c_k	0.5283	p_n	8
c_r	3.864	ψ	0.44Vs
k	1.4	$\tau_{fr,gen,static}$	0.51Nm
R	287 J/(kgK)	$\tau_{fr,gen,vis}$	0.01Nms
Scroll Air Expander		J_{gen}	0.015kgm^2
r	5.5x10^{-3} m	***HAWT***	
ρ_0	9.5x10^{-3} m	A	18.16m^2
δ	4.5x10^{-3} m	ρ	1.225kg/m^3
k_s	0.003183	J_T	2 kgm^2
h	3.33x10^{-2} m	$K_{s,vis}$	0.02Nms
$\tau_{fr,air,static}$	0.307Nm	***Gear Box***	
$\tau_{fr,air,viscous}$	0.0044Nms	η	0.82
A_{in}	4.9x10^{-4} m^2	J_R	0.046 kgm^2
A_{out}	8.52x10^{-5} m^2	J_c	4.15 kgm^2
DC motor		i	5
k_c	0.252 Nm/A	R_0	1.5
L_a	0.78 mH	R_1	1.205
J_{dc}	0.0014 kgm^2	$\tau_{fr,gear,c,static}$	0.174Nm
R_a	0.25 ohm	$\tau_{fr,gear,c,viscous}$	0.0075Nms
$\tau_{fr,dc,static}$	0.3Nm	$\tau_{fr,gear,s,static}$	0.13Nm
$\tau_{fr,dc,viscous}$	7.12x10^{-5}Nms	$\tau_{fr,gear,s,viscous}$	0.0015Nms

APPENDIX B

TABLE III. INERTIAS

Variable	Description
J_k	$iJ_c + \frac{(1+i)^2 J_R}{i}$
J_{k2}	$-\frac{J_k J_s i}{J_R} + J_C$
J_{k3}	$1 - \left(\frac{J_s i^2}{J_R}\right)$
J_{k4}	$\frac{J_s i}{J_R}$
J_{k5}	$\frac{(1+i)J_R}{i} - \frac{J_s J_k}{J_c}(i+1)$
J_{k6}	$-i + J_k/J_c$

References

[1] J. Hansen, M. Sato, P. Kharecha, G. Russell, D. W. Lea, and M. Siddall, "Climate change and trace gases," *Philosophical Transactions of the Royal Society of London A: Mathematical, Physical and Engineering Sciences*, vol. 365, pp. 1925-1954, 2007.

[2] V. Akhmatov, *Analysis of dynamic behaviour of electric power systems with large amount of wind power*: Electric Power Engineering, Ørsted-DTU, Technical University of Denmark, 2003.

[3] X. Luo, J. Wang, M. Dooner, and J. Clarke, "Overview of current development in electrical energy storage technologies and the application potential in power system operation," *Applied Energy*, vol. 137, pp. 511-536, 2015.

[4] A. Cavallo, "Controllable and affordable utility-scale electricity from intermittent wind resources and compressed air energy storage (CAES)," *Energy*, vol. 32, pp. 120-127, 2007.

[5] EUROPEAN COMMISSION, "http://www.uni-saarland.de/fak7/fze//AKE_Archiv/AKE2014H/Vortraege/AKE2014H_04BemtgenEU2014_EnergyStorageStrategyPaper_36p.pdf."

[6] Fichtner, "Erstellung eines Entwicklungskonzeptes Energiespeicher in Niedersachsen," Innovationszentrum Niedersachsen GmbH, Lower-Saxony, Germany2014.

[7] H. Lund, G. Salgi, B. Elmegaard, and A. N. Andersen, "Optimal operation strategies of compressed air energy storage (CAES) on electricity spot markets with fluctuating prices," *Applied thermal engineering*, vol. 29, pp. 799-806, 2009.

[8] B. Mauch, P. Carvalho, and J. Apt, "Can a wind farm with CAES survive in the day-ahead market?," *Energy Policy*, vol. 48, pp. 584-593, 2012.

[9] R. Madlener and J. Latz, "Centralized and Decentralized Compressed Air Energy Storage for Enhanced Grid Integration of Wind Power," *Institute for Future Energy Consumer Needs and Behavior (FCN)*, 2010.

[10] S. Kahrobaee and S. Asgarpoor, "Optimum planning and operation of compressed air energy storage with wind energy integration," in *North American Power Symposium (NAPS), 2013*, 2013, pp. 1-6.

[11] M. V. Dahraie, H. Najafi, R. Azizkandi, and M. Nezamdoust, "Study on compressed air energy storage coupled with a wind farm," in *Renewable Energy and Distributed Generation (ICREDG), 2012 Second Iranian Conference on*, 2012, pp. 147-152.

[12] A. Daneshi, N. Sadrmomtazi, H. Daneshi, and M. Khederzadeh, "Wind power integrated with compressed air energy storage," in *Power and Energy (PECon), 2010 IEEE International Conference on*, 2010, pp. 634-639.

[13] E. Fertig and J. Apt, "Economics of compressed air energy storage to integrate wind power: A case study in ERCOT," *Energy Policy*, vol. 39, pp. 2330-2342, 2011.

[14] N. Hasan, M. Y. Hassan, M. Majid, and H. Rahman, "Mathematical model of compressed air energy storage in smoothing 2MW wind turbine," in *Power Engineering and Optimization Conference (PEDCO) Melaka, Malaysia, 2012 Ieee International*, 2012, pp. 339-343.

[15] H. Ibrahim, A. Ilinca, R. Younes, J. Perron, and T. Basbous, "Study of a hybrid wind-diesel system with compressed air energy storage," in *Electrical Power Conference, 2007. EPC 2007. IEEE Canada*, 2007, pp. 320-325.

[16] H. Sedighnejad, T. Iqbal, and J. Quaicoe, "Performance evaluation of a hybrid wind-diesel-compressed air energy storage system," in *Electrical and Computer Engineering (CCECE), 2011 24th Canadian Conference on*, 2011, pp. 000270-000273.

[17] M. Saadat and P. Y. Li, "Modeling and control of a novel compressed air energy storage system for offshore wind turbine," in *American Control Conference (ACC), 2012*, 2012, pp. 3032-3037.

[18] S. Lemofouet and A. Rufer, "A hybrid energy storage system based on compressed air and supercapacitors with maximum efficiency point tracking (MEPT)," *Industrial Electronics, IEEE Transactions on*, vol. 53, pp. 1105-1115, 2006.

[19] S. Hao, L. Xing, and W. Jihong, "Management and control strategy study for a new hybrid wind turbine system," in *Decision and Control and European Control Conference (CDC-ECC), 2011 50th IEEE Conference on*, 2011, pp. 3671-3676.

[20] S. Hao, L. Xing, and W. Jihong, "Simulation study of energy efficiency for a hybrid wind turbine system," in *Industrial Technology (ICIT), 2013 IEEE International Conference on*, 2013, pp. 781-786.

[21] C. Krupke, J. Wang, J. Clarke, and X. Luo, "Dynamic modelling of a hybrid wind turbine in connection with compressed air energy storage through a power split transmission device," in *Advanced Intelligent Mechatronics (AIM), 2015 IEEE International Conference on*, 2015, pp. 79-84.

[22] Mathworks. (2015, 05/05/2014). *Wind Turbine*. Available: http://uk.mathworks.com/help/physmod/sps/powersys/ref/windturbine.html

[23] A. Rolan, A. Luna, G. Vazquez, D. Aguilar, and G. Azevedo, "Modeling of a variable speed wind turbine with a permanent magnet synchronous generator," in *Industrial Electronics, 2009. ISIE 2009. IEEE International Symposium on*, 2009, pp. 734-739.

[24] FlowBattery. (2015). *Compressed Air Batteries*. Available: http://www.flowbattery.co.uk/compressed-air-batteries

[25] AirSquared. (2015, 30/05/2015). *Oil-free scroll technology*. Available: http://airsquared.com/

[26] J. Wang, X. Luo, L. Yang, L. M. Shpanin, N. Jia, S. Mangan, *et al.*, "Mathematical modeling study of scroll air motors and energy efficiency analysis—part II," *Mechatronics, IEEE/ASME Transactions on*, vol. 16, pp. 122-132, 2011.
[27] J. Wang, L. Yang, X. Luo, S. Mangan, and J. W. Derby, "Mathematical Modeling Study of Scroll Air Motors and Energy Efficiency Analysis—Part I," *Mechatronics, IEEE/ASME Transactions on*, vol. 16, pp. 112-121, 2011.
[28] M. Cai, K. Kawashima, and T. Kagawa, "Power assessment of flowing compressed air," *Journal of fluids engineering*, vol. 128, pp. 402-405, 2006.
[29] H. L. Benford and M. B. Leising, "The lever analogy: A new tool in transmission analysis," SAE Technical Paper1981.
[30] E. Welfonder, R. Neifer, and M. Spanner, "Development and experimental identification of dynamic models for wind turbines," *Control Engineering Practice*, vol. 5, pp. 63-73, 1997.
[31] A. R. Jha, *Wind turbine technology*: CRC press, 2010.
[32] W. Matek, D. Muhs, H. Wittel, and M. Becker, *Roloff/Matek Maschinenelemente: Normung Berechnung Gestaltung*: Springer-Verlag, 2013.
[33] A. M. T. Eastop, *Applied Thermodynamics for Engineering Technologies* vol. 5. Singapore, 1996.
[34] S. Garvey, A. Pimm, J. Buck, S. Woolhead, K. Liew, B. Kantharaj, *et al.*, "Analysis of a Wind Turbine Power Transmission System with Intrinsic Energy Storage Capability," *Wind Engineering*, vol. 39, pp. 149-174, 2015.
[35] The Institute of Engineering Thermophysics Chinese Academy of Sciences. (2015, 27/04/2016). Available: http://www.etp.ac.cn/jgsz/kybm/kybm6/
[36] IMAGES. (2015, 10/10/2015). *Integrated Market-fit and Affordable Grid Scale Energy Storage*. Available: http://www.integratedenergystorage.org/

Christopher Krupke received the B.E. degree in Mechatronics from Coventry University, Coventry, U.K., and the B.E. degree in Mechanical Engineering from the University of Applied Sciences Wolfenbüttel, Germany, in 2012 and 2013, respectively. He is currently a PhD candidate at The University of Warwick, Coventry, U.K., with main research focus on mechatronic systems, energy storage as well as system modelling and control.

Jihong Wang (M'06–SM'09) received the B.E. degree from Wuhan University of Technology, Wuhan, China, the M.Sc. degree from Shandong University of Science and Technology, Shandong, China, and the Ph.D. degree from Coventry University, Coventry, U.K., in 1982, 1985, and 1995, respectively. She is currently a Professor of Power Systems and Control Engineering within the School of Engineering, The University of Warwick, Coventry, U.K. She was a Technical Editor to IEEE Trans. on Mechatronics. Her main research interests include nonlinear system control, system modeling and identification, power systems, energy-efficient acatuators and systems, and applications of intelligent algorithms.

Jonathan Clarke completed his MEng degree in Aeronautical Engineering at Loughborough University in 2008 and achieved his PhD in Avionics also at Loughborough in 2013. Jonathan is currently at the EPSRC Centre for Innovative Manufacturing in Intelligent Automation, with previous work experience as a lab supervisor, project manager and also as a pilot. Research interests include autonomy of expert systems, CNC machine design, compliant actuators and grippers, estimation and control of manufacturing robots, electroadhesion, rapid prototyping and sensor integration from diverse and redundant systems.

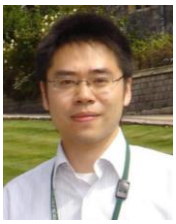

Xing Luo received his B.Eng. degree from Xi'an University of Technology, China, in 2004, the M.Sc. degree from the University of Liverpool, U.K., in 2006, and his Ph.D. degree from the University of Birmingham, U.K. in 2010. Currently, he is a Research Fellow with the School of Engineering, the University of Warwick, UK. His research interests include electrical energy storage, smart grid, engine and pneumatic system modelling and identification, hardware-in-the-loop simulation, energy efficient systems, power electronic systems, real-time control development.